LOCAL STRUCTURE OF TURBULENCE IN STABLY-STRATIFIED BOUNDARY LAYERS

Zbigniew Sorbjan

Department of Physics, Marquette University, Milwaukee, WI 53201, U.S.A.

Accepted to the "Journal of the Atmospheric Sciences" as JAS-1850

Revised on October 14, 2005

Corresponding author address: Department of Physics, Marquette University, 540 North 15th Street, Milwaukee, WI 53201-1881, USA , E-mail: sorbjanz@mu.edu

ABSTRACT

The "flux-based" local scaling in the stably stratified boundary layer is valid only in cases with strong, continuous turbulence, when the gradient Richardson number *Ri* is constant and sub-critical. In order to extend the local similarity approach to cases with weak turbulence (very stable regime), the "gradient-based" local scaling is introduced and discussed in the paper. Both types of local scaling, the "flux-based" and the "gradient-based", are tested based on the data, collected from a 60-m tower during CASES-99. The obtained results show that the "gradient-based" scaling provides a useful framework for the treatment of cases with both strong and weak turbulence and overcritical Richardson numbers.

1. Introduction

The examination of stably-stratified, nocturnal turbulence presents a considerable challenge because of both the theoretical, computational and measuring difficulties. Weak stable turbulence requires very accurate measurements and data analyses (e.g., Vickers and Mahrt, 2005). The stable boundary layer (SBL) often does not reach equilibrium (eg. Caughey et al., 1979; Wyngaard and Kosovic, 1994), and is sensitive to minor influences, such as terrain inclination (e.g., Brost and Wyngaard, 1978, Derbyshire and Wood, 1994), surface heterogeneity (e.g., Mahrt, 1998; Mahrt et al., 1998; Nappo, 1991), and radiative effects, due to the presence of water vapor, water droplets, and aerosols in the atmosphere (e.g., Garrat and Brost, 1981; Duynkerke, 1999; Ha and

Mahrt, 2005; Van de Wiel et al, 2003). Additional complicating factors include meandering motions, development of low-level jets (e.g., Saiki et al, 2000), advection, a variety of density currents and propagating gravity waves, which may cause turbulence by overturning (e.g., Merrill, 1977, Sun et al., 2004).

Standard theories (e.g., Turner, 1973; Yamada, 1975) suggest that turbulence is determined by the gradient Richardson number Ri. Linearized theory predicts that small perturbations in inviscid fluid may grow exponentially for $Ri < Ri_c = 0.25$ (e.g., Miles, 1961, Woods, 1969). In viscid flows this limit may be smaller (Nieuwstadt, 1984). If Ri exceeds the critical value Ri_c, turbulence is suppressed, can decay, or degenerate into wavy motions (e.g., Steward, 1969; Tavoularis and Karnik, 1989). In many geophysical flows, however, turbulent activity exists when Ri is overcritical. Under non-stationary conditions, turbulent mixing may occur at all Richardson numbers (e.g., Schumann and Gerz, 1995).

Recent data analyses indicate that the adequate understanding of the stably-stratified boundary layer (SBL) depends on high-resolution measurements, since turbulence can be confined in layers, sometimes only a few meters deep (e.g., Mahrt and Vickers, 2003; Poulos and Burns, 2003). Similarly, large-eddy simulations imply that the accurate description of the SBL requires very fine-resolution (about 1 m) calculations (e.g., Beare and MacVean, 2004). Thin layers in the SBL can have a step-like structure, with small and large eddies (e.g., Chimonas, 1999). Basley et al. (2003) detected thin layers with temperature gradients of 28 K/m.

The interactions between waves and turbulence in the SBL have been well documented during the past few decades (e.g., Hunt et al. 1985, Finnigan and Enaudi,

1981; King et al 1987, Sun et al., 2004). Shutts et al. (1988) found large amplitude gravity waves in the lower atmosphere, providing a large dynamic Reynolds stress, one order of magnitude larger than that in typical stable conditions. King et al. (1987) described waves, which propagate down to the earth's surface from a height about 1 km. Rees and Mobbs (1988) identified topographically generated wavy modes. Blumen et al. (2001) reported cases of shear instability with trains of billows, resembling a cat's eye pattern, embedded within step-like structures.

Turbulence in the SBL can have either "continuous" or "intermittent" (sporadic) character (Mahrt et al., 1998). Continuous turbulence takes place during cloudy nights with strong winds. Its presence is manifested by a relatively large, negative heat flux at the surface, which decreases with height. On the other hand, the intermittent turbulence is characterized by short burst of fluctuations followed by events with low turbulent activity (e.g., Mahrt, 2003, Mahrt and Vickers, 2005). It occurs with clear, nocturnal skies, and weak winds.

Intermittence can take the form of "fine-scale intermittence", when only small-scale turbulence is present, or "global intermittence", when turbulence on all scales collapses (e.g., Mahrt, 2003). Intermittence could be interrupted by local shear effects (e.g., Sun et al., 2004), by turbulence generated aloft and diffused to the surface, by locally generated waves, gravity currents (e.g. Coulter, 1990, Poulos, 2002, Nappo, 1991), or by convection generated by radiative cooling at the tops of stratocumuli clouds (e.g., Lilly and Schubert, 1980). Knowledge of physical mechanisms behind the intermittent behavior of turbulence in SBL is still limited.

Many authors (e.g., Mahli, 1995, Oyha et al, 1997, Mahrt 1998, Mahrt et al. 1998)

categorize the SBL into either weakly stable, or very stable regimes. The definitions of these regimes vary among studies. The weakly stable regime is often defined as the case with the Richardson number $Ri < 0.25$, with significant wind shear, clouds, and continuous turbulence near the surface.

In contrast, the very stable regime is characterized by small shear, clear skies, $Ri > 0.25$, and intermittent turbulence. The very stable regime may assume an "upside-down" character, with the strongest turbulence at the top of the surface inversion layer, where it is generated by vertical shear on the underside of the lower-level jet stream . The upper portion of the SBL can be detached from the nearly laminar surface sub-layer. The detachment may be only temporary, since flow acceleration above the very stable surface layer may lead to shear generation of turbulence, and recoupling of elevated turbulence with the surface (e.g., Businger, 1973). The very stable boundary layer is often layered, and its depth may not be well defined (e.g., Mahrt et al.,1998).

Currently, there is no accepted theory of the SBL that would generally treat the described above properties of the SBL. Nevertheless several theoretical developments, obtained within the last five decades, deserve mention. Among them is the first constructive theoretical description of stable turbulence in the atmospheric surface layer, proposed by Monin and Obukhov (1954) within their similarity theory. Another milestone is the introduction of local scaling, based on dry, second-order closure equations by Nieuwstadt (1984). Sorbjan (1986, a, b, c) developed local similarity functions based on dimensional analysis and a similarity approach.

Each of the above listed theories was found to have limitations. The Monin-Obukhov similarity can be applied only to the surface layer. Nieuwstadt's local theory,

based on the "flux-based" local scaling, is valid only during continuous turbulence, in the quasi steady-state, for which the heat flux is linear with height. Sorbjan's local approach, in which the heat flux is allowed to be non-linear with height, is more general but it also lacks consistency, when the Richardson number varies with height, and also outside the critical limit.

The purpose of this paper is to further extend the local similarity approach by introducing an alternate, "gradient-based" scaling, intended to be valid in both the weakly stable and very stable conditions. The paper has the following structure. First, "flux-based" local scaling is briefly be reviewed in Section 2. Next, the "gradient-based" scaling is introduced and discussed. In Section 3, both types of scales are examined, based on data obtained during the CASES-99 field experiment.

2. Local scaling

Nieuwstadt (1984) derived his local scaling by employing a steady-state, dry model of the SBL. His original system consisted of seven, second-order moment equations, which are listed in the Appendix. By eliminating the vertical heat flux in the considered system, and using the generalized Monin-Obukhov length $\Lambda(z)$, Nieuwstadt obtained:

$$\frac{\tau^{1/2}\Lambda}{K_M} - \frac{1}{\kappa} - C_\varepsilon \frac{e^3}{\tau^{3/2}} \frac{\Lambda}{l} = 0$$

$$\frac{2}{3} C_2 \frac{\tau^{1/2}\Lambda}{K_M} - \frac{1}{\kappa}(2 + \frac{4}{3} C_3) - \frac{2}{3} C_\varepsilon \frac{e^3}{\tau^{3/2}} \frac{\Lambda}{l} - C C_\varepsilon \frac{e}{\tau^{1/2}} \frac{\Lambda}{l} (\frac{\overline{w^2}}{\tau} - \frac{e^2}{3\tau}) = 0$$

$$\left[(1-C_2)\frac{\overline{w^2}}{\tau}-\frac{C_1}{2}\frac{e^2}{\tau}\right]\frac{\tau^{1/2}\Lambda}{K_M}+\frac{1}{\kappa}(1+C_3)\frac{H}{\overline{w\theta}}-CC_\varepsilon\frac{e}{\tau^{1/2}}\frac{\Lambda}{l}=0$$

$$\frac{\overline{w^2}}{\tau}\frac{\tau^{1/2}\Lambda}{K_H}-\frac{1}{\kappa}(1-a_1)\frac{\overline{\theta^2}\tau}{\overline{w\theta}^2}-dC_\varepsilon\frac{e}{\tau^{1/2}}\frac{\Lambda}{l}=0 \qquad (1)$$

$$\frac{\tau^{1/2}\Lambda}{K_H}-C_\theta C_\varepsilon\frac{e}{\tau^{1/2}}\frac{\Lambda}{l}\frac{\overline{\theta^2}\tau}{\overline{w\theta}^2}=0$$

$$\frac{\tau^{1/2}\Lambda}{K_H}+\frac{1}{\kappa}(1+a_2)\frac{\tau^{1/2}\Lambda}{K_M}+dC_\varepsilon\frac{e}{\tau^{1/2}}\frac{H}{\overline{w\theta}}\frac{\Lambda}{l}=0$$

where $\Lambda(z) = -\tau^{3/2}/(\kappa\beta\overline{w\theta})$, κ is the von Karman constant, and all other terms are described in the Appendix.

Nieuwstadt argued that the above six equations express a relationship between seven dimensional combinations $K_M/\tau^{1/2}\Lambda$, $K_H/\tau^{1/2}\Lambda$, $\overline{w^2}/\tau$, e^2/τ, $H/\overline{w\theta}$, $\overline{\theta^2}\tau/\overline{w\theta}^2$, and l/Λ. If the mixing length is assumed to be linear: $l \sim z$, then the dimensional combinations should depend only on the dimensionless height z/Λ:

$$K_M/\tau^{1/2}\Lambda \sim K_H/\tau^{1/2}\Lambda \sim \overline{w^2}/\tau \sim e^2/\tau \sim H/\overline{w\theta} \sim \overline{\theta^2}\tau/\overline{w\theta}^2 = f(z/\Lambda) \qquad (2)$$

In the limit of $z/\Lambda \to \infty$, the mixing length becomes limited, and the set (1) no longer contains z as a variable (the z-less regime). As a consequence, the dimensionless quantities in (2) approach constant values:

$$K_M/\tau^{1/2}\Lambda \sim K_H/\tau^{1/2}\Lambda \sim \overline{w^2}/\tau \sim e^2/\tau \sim H/\overline{w\theta} \sim \overline{\theta^2}\tau/\overline{w\theta}^2 = const \qquad (3)$$

Nieuwstadt limited his discussion to the dry, quasi steady-state case, for which $\overline{w\theta}/\overline{w\theta}_o = (1 - z/h)$, and $\tau/\tau_o = (1 - z/h)^{3/2}$, where h is the height of the SBL. This approach neglects the effects of radiative fluxes in the SBL, and leads to the singularity of temperature at the top of the SBL (e.g., Sorbjan, 1987, Derbyshire, 1990). Sorbjan (1987) argued that in a more general case, which includes the effects of radiative cooling and advection, $\overline{w\theta}/\overline{w\theta}_o = (1 - z/h)^a$ and $\tau/\tau_o = (1 - z/h)^b$, where a and b are empirical constants. The singularity of temperature at the top of the SBL is avoided, when $a \geq b$ (Sorbjan, 1987).

Sorbjan's (1986a, b, c) approach was based on dimensional analysis. It recognized that the semi-empirical similarity functions, expressed in terms of the Monin-Obukhov scales in the surface layer (i.e., u_* for wind velocity, $t_* = -\overline{w\theta}_o/u_*$ for temperature, $q_* = -\overline{wq}_o/u_*$ for humidity, and $L = u_*^2/[\kappa \beta t_*]$ for height) must be identical with the universal functions, scaled by the analogous local scales:

$$
\begin{aligned}
U_*(z) &= \tau^{1/2} \\
T_*(z) &= -\overline{w\theta}/U_* \\
Q_*(z) &= -\overline{wq}/U_* \\
\Lambda(z) &= U_*^2/(\kappa\beta T_*)
\end{aligned}
\qquad (4)
$$

where $\overline{wq}$ is the humidity flux and $Q_*(z)$ is the humidity local scale. Consequently, any scaled statistical moment X is expected to be independent of height in the stable boundary layer:

$$\frac{X}{U_*^a T_*^b Q_*^c \Lambda^d} = const \qquad (5)$$

where *a, b, c,* and *d* are appropriate power coefficients.

The above hypothesis was found to be valid for gradients, variances, covariances, eddy viscosities and diffusivities, dissipation rates, structure parameters C_v^2, C_T^2, spectra and cospectra only in the continuous, sub-critical case (e.g., Sorbjan, 1995). Note that (5) implies that the gradient Richardson number $Ri = N^2 / S^2 \sim (\beta T_*/\Lambda) / (U_*/\Lambda)^2 = const$, where $N = (\beta\, d\Theta/dz)^{0.5}$ is the Brunt-Vâisâlâ frequency, and $S = [(\partial U/\partial z)^2 + (\partial V/\partial z)^2]^{1/2}$ is the wind shear.

The local similarity based on (4) and (5) is invalid, when the Richardson number varies with height, and also outside the critical limit. Moreover, it fails in the intermittent case near the Earth's, when $\overline{w'\theta'} \sim 0$, $\overline{u'w'} \sim 0$. The temperature gradient in this case cannot be accurately defined: $d\Theta/dz \sim T_*/\Lambda \sim \beta\, \overline{w\theta}^2 / \overline{u'w'} \sim 0/0$. This drawback of the Monin-Obukhov scaling can be associated with the fact that the z-less regime is locally shear generated, and not systematically coupled to the surface. When the proximity to the surface is sufficiently small, turbulence can be controlled by radiative effects, i.e., the long-wave flux cooling can exceed the sensible heat flux divergence (Mahrt and Vickers, 2005).

Additional disturbing effects can be related to large flux errors, which contaminate the similarity scales. Fluxes computed from traditional methods for weak turbulence are erratic and often of either sign because random flux errors are larger than the magnitude of the true flux (e.g., Mahrt and Vickers, 2005). Because the stability

parameter z/Λ is a function of the turbulence itself, serious self-correlation errors can also appear (Mahrt et al., 1998; Mahrt and Vickers, 2005). Finally, in very stable regime, fluxes and variances can be influenced by non-turbulent motions, which do not follow the Monin-Obukhov scaling laws (e.g., Mahrt et al., 1998).

In an attempt to extend the validity of the local similarity approach, let us propose the following alternative local scaling (Sorbjan, 2001):

$$\begin{aligned} U_n(z) &= \sigma_w \\ L_n(z) &= U_n/N \\ T_n(z) &= L_n d\Theta/dz \\ Q_n(z) &= L_n dq/dz \end{aligned} \tag{6}$$

where σ_w^2 is the vertical velocity variance and N is the Brunt-Våisålå frequency. The length scale L_n in (6) can be derived from a simple energy budget, in which the potential energy $E_p \sim \beta\, d\Theta/dz\, L_n^2$, acquired by a portion of fluid displaced by a vertical distance L_n, is equated with its initial kinetic energy $E_k \sim \sigma_w^2$ (e.g., Pristley, 1958, Mahrt, 1979, Hunt et al., 1988, Mahrt et al., 1998). It can be noted, that analogous scales were previously employed to describe the dynamics of the stably stratified interfacial layer above the mixed layer (Sorbjan, 2004), with $\sigma_w \sim w_*$, where w_* is the convective scale for velocity.

Applying the local scales (6) to the set (A1), together with a closure assumption that the mixing length $l \sim L_n$, yields:

$$\frac{\tau}{U_n^{\,2}} + \frac{\overline{w\theta}}{U_n T_n} Ri^{1/2} - C_\varepsilon \frac{e^3}{U_n^{\,3}} Ri^{1/2} = 0$$

$$\frac{2}{3} C_2 \frac{\tau}{U_n^{\,2}} + (2 + \frac{4}{3} C_3) \frac{\overline{w\theta}}{U_n T_n} Ri^{1/2} - \frac{2}{3} C_\varepsilon \frac{e^3}{U_n^{\,3}} Ri^{1/2} - CC_\varepsilon \frac{e}{U_n} Ri^{1/2} (1 - \frac{e^2}{3U_n^{\,2}}) = 0$$

$$\left[(1 - C_2) - \frac{C_1}{2} \frac{e^2}{U_n^{\,2}} \right] Ri^{1/2} - (1 + C_3) \frac{H}{U_n T_n} - CC_\varepsilon \frac{e\tau}{U_n^{\,3}} = 0$$

$$1 - (1 - a_1) \frac{\overline{\theta^2}}{T_n^{\,2}} + dC_\varepsilon \frac{e}{U_n} \frac{\overline{w\theta}}{U_n T_n} = 0 \qquad (7)$$

$$\frac{\overline{w\theta}}{U_n T_n} + C_\theta C_\varepsilon \frac{e}{U_n} \frac{\overline{\theta^2}}{T_n^{\,2}} = 0$$

$$\frac{\tau}{U_n^{\,2}} - (1 + a_2) \frac{\overline{w\theta}}{T_n U_n} Ri^{1/2} - dC_\varepsilon \frac{e}{U_n} \frac{H}{T_n U_n} = 0$$

The above system implies that the dimensionless combinations in (7) are functions of a local gradient Richardson number *Ri:*

$$\overline{w\theta} / (U_n T_n) \sim H/(U_n T_n) \sim \overline{\theta^2} / T_n^{\,2} \sim e^2 / U_n^{\,2} \sim \tau / U_n^{\,2} = f(Ri) \qquad (8)$$

Because the eddy diffusivities have been eliminated in (7), the length scale L_n is absent in (8).

Based on (8), it can be argued that generally, any scaled statistical moment X in the SBL is expected to be a function of a local Richardson number:

$$\frac{X}{U_n^a T_n^b Q_n^c L_n^d} = f_x(Ri) \qquad (9)$$

where *a, b, c,* and *d* are appropriate power coefficients.

A similar result can be obtained based on dimensional analysis and similarity approach (e.g., Sorbjan, 1995). Considering 5 governing parameters of stable turbulence: $\beta = g/T_o$, $d\Theta/dz$, dq/dz, $S = [(\partial U/\partial z)^2 + (\partial V/\partial z)^2]^{1/2}$, and σ_w (which involve 4 independent units [m, s, K, kg]), yields 4 scales listed in Eqs. 6, and one dimensionless parameter - the gradient Richardson number *Ri* (Sorbjan, 2005).

Turbulence described by the system (7) is assumed to be stationary. Consequently, one can expect that (9) is valid in the steady state. In some cases of non-stationarity, the effects could be parametrically included in (9) through the local Richardson number (e.g., Schumann and Gerz, 1995).

It can be noted that during continuous turbulence, when $Ri = \text{const} < Ri_c$, both scaling sets, (4) and (6), are equivalent. Indeed, based on (5) we have: $d\Theta/dz \sim T_*/\Lambda \sim \beta\, \overline{w\theta}^2/\tau^2$. On the other hand, from (8), we have: $\overline{w\theta}^2 \sim U_n^2 T_n^2 \sim d\Theta/dz\ \sigma_w^4/\beta$, which gives (with $\tau \sim \sigma_w^2$) the same relationship between the temperature gradient and the temperature flux. From (8), we will also obtain that $\Lambda \sim \tau^{3/2}/(\beta\, \overline{w\theta}) \sim \sigma_w/N = L_n$. Mason and Derbyshire (1990), Derbyshire (1990), Hunt et al. (1985) reported a close association between Λ and L_n based on measurements in the weakly stable case.

There are several practical advantages of using the gradient-based scaling (6) versus employing the flux-based scaling (4). First of all, the velocity scale U_n, defined by the vertical velocity variance, is less sensitive to the sampling problems**.** Moreover, U_n is quite robust, since the vertical velocity variance is less sensitive to the choice of averaging time scale compared to other moments (e.g., Mahrt and Vickers, 2005). U_n is

less vulnerable to sampling problems, compared to flux-based quantities. Its probability distribution is relatively independent of *Ri* (e.g., Mahrt and Vickers, 2005). The length scale L_n does not inherit the difficulty of measuring fluxes in the very stable case. At the same time, the measurements of scalars seem to be more accurate than the evaluation of their fluxes, even though an appropriate calculating of their gradients requires a sufficient vertical resolution of observations. The effects of multiple layers within the SBL can be included and parametrically expressed in terms of the Richardson number *Ri*, which can vary with height, and can be larger than Ri_c.

3. Empirical verification

In this Section, both sets of scales, the "flux-based" (4) and the "gradient-based" (6) will be tested based on atmospheric data, presented by Mahrt and Vickers (2005). The considered data set was collected during the CASES-99 experiment in October of 1999. The experimental site was located over grassland in south central Kansas (Poulos et al., 2002).

Data collecting and processing procedures can be summarized as follows (Mahrt and Vickers, 2005). Sonic anemometer data sets were obtained on 6 levels of a 60-m tower. Profiles of mean temperature were computed from 34 thermocouples on the 60-m tower (Burns and Sun, 2000). In addition, data from the 1.5-m and 5-m levels of a mini tower, 10 m to the side of the main tower, were included. Data was quality controlled and pre-processed following the procedure of Vickers and Mahrt (1997, 2005). The applied corrections for sonic tilt are outlined in Mahrt et al. (2000). Perturbations were defined as

deviations from a record-dependent averaging length. Covariances were averaged over one hour to reduce flux sampling errors, except for time-height cross-sections, for which 30 minute-averages were used. Mostly cloudy cases were removed by discarding records, where the magnitude of the surface net radiation loss was less than 40 W/m^2. Finally, the composite profiles for the strong S and weak W turbulence classes were computed.

The strong-turbulence composite set S was based on 1-hour records, collected on day 284 (11 October 1999), beginning at the hours of 1, 2, 3, 4, 5, and 6 (Central Standard Time), on day 298 (hours 2, 3, and 4), and on day 300 (hours 22, 23, and 0). The weak-turbulence composite set W was based on records collected on day 290 (hours: 21, 22, and 23), on day 291 (hours: 4, 17, 18, and 19), on day 292 (hours: 4, 6, 20, 21, and 23), on day 293 (hours: 0, and 1), on day 296 (hour 23), on day 298 (hours: 18, and 19), on day 299 (hours: 1, 2, and 4), on day 301 (hours: 5 and 19). The composite profiles are not equivalent to those composed based on ensemble averaging.

The surface-layer characteristics of both composite cases are depicted in Table 1. The surface-layer scales u_*, T_*, L in the table were evaluated based on observations at z = 1 m. The net radiation flux, $F_n = F\downarrow - F\uparrow$, was calculated as an average for four radiation stations (stations 1, 2, 3, and 5) surrounding the main tower (e.g., Sun et al. 2003). Using near neutral observations, the roughness length (for momentum) at the site was estimated to be z_o = 2.7 cm. As seen in the table, the surface temperature flux H_o, defined by the product $(-u_*T_*)$, is about 12 times larger in case S than in case W. The Monin-Obukhov height L in case S is about 40 times larger than in case W.

A general characteristic of the considered composite cases is presented in Figures 1-3. Note that the temperature in Figure 1 is obtained as the deviation from the surface value. The standard errors for all moments can be found in Mahrt and Vickers (2005). The error

bars are not shown in the figures presented in this paper in order to indicate that local scaling was applied to the processed data.

Based on Figures 1-3, one might conclude that case W is characterized by a larger temperature difference between the top and the bottom of the tower, lesser wind velocity, and consequently weaker turbulence. The R ichardson number exceeds the critical value. The surface heat flux is relatively small, and the SBL is relatively shallow. In case S, the temperature difference between the top and the bottom of the tower is smaller, the wind velocity greater, which produces stronger turbulence. The Richardson number is below the critical value. The surface heat flux is larger than in case W. In case S, observations contain only a part of the boundary layer.

The "flux-based" scaling (4) is tested in Figures 4 and 5. The figure depicts the dimensionless variances, $\overline{\theta^2}/T_*^2$ and $\overline{w^2}/U_*^2$, as the function of the dimensionless height z/Λ. In case S, the observational points are confined to the portion of the plot, where z/Λ is small (< 2.5). In case W, the observational points are located in the region where z/Λ > 1.9. It can be noted that the larger values of the parameter z/Λ in case W are due to the smaller values of the Reynolds stress (as seen in Figure 3b).

The dimensionless temperature variance in Figure 4a is nearly constant with the dimensionless height in case S (which agrees with Eq. 5), and is highly scattered in case W. A possible dependence between the dimensionless variance $\overline{\theta^2}/T_*^2$ and z/Λ is represented by the dotted line in the figure. The constant value of the temperature variance in case S ($z/\Lambda < 3$) can be estimated as 4.5, which gives $\sigma_\theta/T_* \sim 2.1$. This value can be compared with the result of Nieuwstadt (1984), who obtained $\sigma_\theta/T_* \sim 3$.

Figure 4a indicates that the "flux-based" scaling (4) is effective and consistent

with Eq. 5 in case S, and it is ineffective in case W. A similar conclusion follows from Figure 4b, where the dimensionless vertical velocity variance is shown to be nearly constant in case S. The constant value of $\overline{w^2}/U_*^2$ in the figure can be estimated as 2.5, which gives $\sigma_w / U_* \sim 1.4$. The same result was obtained by Nieuwstadt (1984). The vertical velocity variance in case W increases with the dimensionless height z/Λ in a quite consistent manner (i.e., without any significant scatter). Large values of both dimensionless variances in Figures 4a and 4b imply that the flux-based local scales T_* and U_* are relatively small at large z/Λ.

The dependence between the dimensionless height z/Λ and the Richardson number Ri is shown in Figure 5. In case S, when $z/\Lambda \rightarrow 0$, then the Richardson number Ri also decreases to zero. On the other hand, in the range of z/Λ from about 1 to 3 (which is the "flux-based" local scaling regime, described by Eq. 5), Ri is approximately constant, and equal to 0.15. Nieuwstadt (1984) obtained $Ri \sim 0.2$ in the same range of z/Λ. In case W, which is confined in figure in the range of z/Λ from about 2 to about 760, the Richardson number Ri increases from about 0.5 to about 5.4. Consequently, since Ri varies with heigh, the “flux-based” scaling (4) is clearly inconsistent in this case.

The “gradient-based” scaling (6) is examined in Figures 6a-c. Figure 6a shows the dimensionless temperature flux $\overline{w\theta}/(U_n T_n)$ as a function of the Richardson number. As expected, the dimensionless temperature flux vanishes in the neutral limit, when $Ri \rightarrow 0$. On the other hand, when the temperature stratification becomes sufficiently large, turbulence is suppressed, and the dimensionless temperature flux decreases. At some value of Ri between these two limiting regimes (which is about 0.25 in the Figure), the dimensionless temperature flux reaches a minimum, equal to about -0.3. A similar

minimum was detected by Mahli (1995) at about z/L = 0.2 (according to Businger, 1973, this value is equivalent to $Ri \sim 0.1$), and Pahlow et al. (2001) at z/L = 0.1. Mahrt et al. (1998), obtained $\overline{w\theta}$ = -0.045 K m/s at about z/L = 0.065 (which is equivalent to $Ri \sim$ 0.065). The authors argued that the abscissa (i.e., z/L or Ri), for which the flux reaches minimum defines a threshold between weakly stable and very stable regime**.**

The presence of the minimum in Figure 6a indicates that the value of the dimensionless temperature flux in the SBL is bounded: $\overline{w\theta}(z) \geq -0.3\ U_n T_n$, for any z and any *Ri*. Derrbyshire (1990) found another upper stability bound for the surface flux $\overline{w\theta}_o \geq H_m \sim -G^2 f/\beta$, where *G* is the geostrophic wind, *f* is the Coriolis parameter, and β is the buoyancy parameter. His formula implies that the surface flux is limited by a product of the velocity scale equal to *G*, and the temperature scale equal to Gf/β. Contrary to our result, such a temperature scale is independent of the temperature stratification near the surface.

The dimensionless Reynolds stress τ/U_n^2 is presented in Figure 6b. As the temperature stratification vanishes in the neutral case, when $Ri \rightarrow 0$, the value of the Reynolds stress reaches a constant value. When the temperature stratification becomes sufficiently large and $Ri \rightarrow \infty$, turbulence is suppressed, and the dimensionless stress decreases. The values of the dimensionless stress, presented by Schumann and Gerz (1995) in the range $Ri < 0.5$ (based on laboratory data), show a faster drop-off, from $\tau/U_n^2 \sim 0.75$ - 0.95 at $Ri = 0$, to about 0.2 at $Ri = 0.5$.

Figure 6c shows the dependence of the dimensionless temperature variance $\overline{\theta^2}/T_n^2$ on the Richardson number. As in Figure 5a, the temperature variance vanishes,

when $Ri \rightarrow 0$. The temperature variance decreases, when $Ri \rightarrow \infty$. At some value of Ri between these two limiting regimes (which is $Ri \sim 1$ in the figure), the dimensionless temperature variance reaches a maximum, equal to about 1.5. A similar maximum of the dimensionless temperature variance was detected by Mahrt et al (1998), who obtained $\sigma_\theta / t_* = 2$ at about $z/L = 0.1$ (according to Businger (1973) this value is equivalent to $Ri = 0.05$). The presence of the maximum indicates that $\overline{\theta^2}(z) \leq 1.5\, T_n^2$, for any level z within the SBL, and for any value of Ri.

Finally, Figure 7 illustrates the dependence of the correlation coefficient $r_{w\theta}$, between the temperature and vertical velocity, on the Richardson number. The curve in the figure (and also the curves in Figures 4-6) have a tentative (subjective) character. The correlation coefficient is about -0.35 in the neutral limit, when $Ri \rightarrow 0$, and slowly increases, when $Ri \rightarrow \infty$. The results presented by Shumann and Gerz (1995) in the range $Ri < 0.5$ (based on laboratory experimental data) reflect a faster drop-off in $r_{w\theta}$, from about -0.5 at $Ri = 0$ to about -0.1 at $Ri = 0.5$.

4. Final remarks

Stably-stratified shear flows exist in the stratosphere, troposphere, in the atmospheric boundary layer over colder (during warm air advections), or radiatively cooled surfaces, and in the ocean. Although numerous studies have examined various aspects of stably-stratified flows, a unified theory of this case has been missing, partly due to measuring difficulties of weak turbulence, and partly due to a variety of complicating physical processes in the SBL. Lately, progress in understanding of stable

turbulence has been achieved, based on recent field campaigns, such as STABLES-98 (Cuxart et al., 2000), and CASES-99 (Paulos et al., 2002). In the present paper, the CASES-99 observations have been used in order to evaluate local similarity approach for the description of stably-stratified shear flows.

Two composite data sets (referred to as W and S), obtained during CASES-99, have been employed. Case W is characterized by weak turbulence, small surface heat flux, and the local Richardson numbers, exceeding its critical value. In case S, turbulence is stronger, and the local Richardson numbers are below the critical value. The considered sets used to examine two types of local scaling, the "flux-based" and "gradient-based".

The analysis has shown that the "flux-based" local scaling is effective in case S, and ineffective in case W. Generally, the "flux-based" local scaling is valid only in cases with strong, continuous turbulence, when the gradient Richardson number Ri is constant and sub-critical. It fails in the intermittent case, when the fluxes are small. It is also known to introduce self-correlation errors, i.e., the scaled variables and the stability parameter z/L_* depend on surface fluxes.

The "gradient-based" scaling produces consistent results in both cases, W and S, with dimensionless parameters dependent on the Richardson number. This could be related to the advantageous properies of the "gradient-based" scales. The velocity scale U_n, defined by the vertical velocity variance, is less sensitive to sampling problems, compared to the flux-based scale. It is more robust, because the vertical velocity variance is relatively less sensitive to the choice of an averaging time-scale, and its probability distribution is nearly independent of Ri. The length scale L_n does not inherit the difficulty

of measuring fluxes. The "gradient-based" scales are equivalent to the "flux-based" scales in the case when the Richardson number is sub-critical and constant with height..

Concluding, the "gradient-based" scaling provides a useful framework for examining stably-stratified shear turbulence. Effects of non-stationarity and multiple layers within the SBL can be included and parametrically expressed in terms of the Richardson number Ri, which can vary with height, and can be larger than Ri_c. The evaluation of the SBL height h is irrelevant in this approach.

APPENDIX

The original system employed by Nieuwstadt (1984) consisted of seven dry, steady-state, second-order moment equations, modified by additional assumptions that the stress, the velocity gradient, and the horizontal heat flux are parallel. The set included equations for the turbulent kinetic energy $E = e^2/2$, the vertical velocity variance $\overline{w^2}$, the modulus of the Reynolds stress τ, the vertical heat flux $\overline{w\theta}$, the horizontal heat flux H, and the temperature variance $\overline{\theta^2}$:

$$\tau S + \beta\overline{w\theta} - C_\varepsilon \frac{e^3}{l} = 0$$

$$\frac{2}{3}C_2\tau S + (2 + \frac{4}{3}C_3)\beta\overline{w\theta} - \frac{2}{3}C_\varepsilon \frac{e^3}{l} - CC_\varepsilon \frac{e}{l}(\overline{w^2} - \frac{e^2}{3}) = 0$$

$$\left[(1 - C_2)\overline{w^2} - \frac{C_1}{2}e^2\right]S - (1 + C_3)\beta H - CC_\varepsilon \frac{e\tau}{l} = 0$$

$$-\overline{w^2}\frac{\partial\theta}{\partial z} + (1 - a_1)\beta\overline{\theta^2} - dC_\varepsilon \frac{e}{l}\overline{w\theta} = 0 \qquad \text{(A1)}$$

$$-\overline{w\theta}\frac{\partial\theta}{\partial z} - C_\theta C_\varepsilon \frac{e}{l}\overline{\theta^2} = 0$$

$$\tau\frac{\partial\theta}{\partial z} - (1+a_2)\,\overline{w\theta}\,S - d\,C_\varepsilon \frac{e}{l}H = 0$$

where $\tau = (\overline{uw}^2 + \overline{vw}^2)^{1/2}$, $\tau = K_M S$, $S = [(\partial U/\partial z)^2 + (\partial V/\partial z)^2]^{1/2}$ is the wind shear, $\overline{w\theta} = -K_H \partial\Theta/\partial z$, $H = [\overline{u\theta}^2 + \overline{v\theta}^2]^{1/2}$, $\beta = g/T$ is the buoyancy parameter, l is the mixing length, K_M and K_H are the eddy viscosity and diffusivity, and a_1, a_2, d, C, C_1, C_2, C_3 ,C_q, C_e are constants.

Acknowledgments

The performed research has been supported by the National Science Foundation grant No. ATM-0400590. The author's appreciation is directed to Drs. Larry Mahrt and Dean Vickers of Oregon State University for providing both data sets, and also for their helpful suggestions and informative discussions.

References

Balsley, B.B., R.G. Frehlich, M.L. Jensen, Y. Meillier, and A. Muschinski, 2003: Extreme gradients in the nocturnal boundary layer: structure, evolution and potential causes. *J. Atmos. Sci,* **60**, 2496-2508.

Beare, R.J. and M.K. Macvean, 2004: Resolution sensitivity and scaling of large-eddy simulations of the stable boundary layer. *Bound.- Layer Meteor.,* **112**, 257-281.

Blumen, W., R. Banta, S.P. Burns, D.C. Fritts, R. Newsom, G.S. Poulos, J. Sun, 2001: Turbulence statistics of a Kelvin-Helmholtz billow event observed in the night-time boundary layer during the Cooperative Atmosphere-surface exchange study field program. *Dyn. Atmos. Oceans*, **34**, 189-204.

Brost, R. A., and J. C. Wyngaard, 1978: A model study of the stably stratified planetary boundary layer., *J. Atmos. Sci.,* **36**, 1041 - 1052.

Businger, J.A., 1973: Turbulent transfer in the atmospheric surface layer. In: *Workshop on Micrometeorology*. Ed. D.A. Haugen. American Meteorological Society.

Caughey, S.J., J.C. Wyngaard, and J.C. Kaimal, 1979: Turbulence in the evolving stable boundary layer. *J. Atmos. Sci.,* **36**, 1041 - 1052.

Chimonas, H., 1999: Steps, waves and turbulence in the stably stratified planetary boundary layer. *Bound.- Layer Meteor.,* **90**, 397-421.

Coulter, R.L., 1990: A case study of turbulence in the stable nocturnal boundary layer. *Bound. -Layer Meteor.,* **52**, 75-92.

Cuxart, J., C. Yague, G. Morales, E. Terradellas, J. Orbe, J. Calvo, A. Fernandez, M. R. Soler, C. Infante, P. Buenestado, A. Espinalt, H. E. Joergensen, J. M. Rees, J. Vila, J. M. Redondo, I. R. Cantalapiedra, and L. Conangla, 2000: Stable atmospheric boundary layer experiment in Spain (SABLES, 98): A report. *Bound. -Layer Meteor.,* **96**, 337-370.

Derbyshire, S.H., 1990: Nieuwstadt's stable boundary layer revisited. *Quart. J. Roy. Meteorol. Soc.,* **116**, 127-158.

Derbyshire, S.H. and N.Wood, 1994: The sensitivity of stable boundary layers to small slopes and other influences. In: *Stably Stratified Flows: Flow and Dispersion over*

Topography. Clarendon Press.

Duynkerke, P.G., 1999: Turbulence, radiation and fog in Dutch stable boundary layers. *Bound.- Layer Meteor.*, **90**, 447-477.

Finnigan, J.J. and F. Enaudi 1981, Interaction between an internal gravity wave and the PBL. *Quart. J. Roy. Meteor. Soc.,* **107**, 807-832.

Garrat, J.R. and R.A. Brost, 1981: Radiative cooling within and above the nocturnal boundary layer. *J. Atmos. Sci.*, **38**, 27-30-2746.

Ha, K-J., L. Mahrt, 2003, Radiative and turbulent fluxes in the nocturnal boundary layer. *Tellus*, **55A**, 317-327.

Hunt, J.C.R., J.C. Kaimal, and J.E. Gaynor, 1985: Some observations of turbulence structure in the stable layers. *Quart. J. Roy.Meteor. Soc.*, **92**, 793-815.

Hunt, J.C.R., D.D. Strech, and R.E.Britter, 1988: Length scales in stably stratified turbulent flows and their use in turbulent models. *Stably Stratified Flows and Dense Gas Dispersion*, J.S. Puttok. Ed., Clarendon Press, 285-321.

King, J.C., S.D. Mobbs, M.S. Darby, and J.M.Reeds, 1987: Observation of an internal gravity wave in the lower troposphere at Halley, Antarctica. *Bound.-Layer. Meteor.,* **39**, 1-14.

Lilly, D.K and W.H. Schubert, 1980: The effects of radiative cooling in a cloud-topped mixed layer. *J. Atmos. Sci.,* **37**, 482-487.

Mahli, Y.S.,1995: The significance of the dual solutions for heat fluxes measured by the temperature fluctuation method in stable conditions. *Bound.-Layer Meteor.*, **74**, 389-396.

Mahrt, L., 1979: Penetrative convection at the top of a growing boundary layer.

Quart. J. Roy. Meteorol. Soc., 105, 469-485.

Mahrt, L., 1998: Stratified atmospheric boundary layers and breakdown of models, *J. Theor. Comp. Fluid. Dyn.*, **11**, 263-280.

Mahrt, L., X. Lee, A. Black, H. Neumann and R. M. Staebler, 2000: Vertical mixing in a partially open canopy. *Ag. and For. Meteorol.,* **101**, 67-78.

Mahrt, L., J. Sun, W. Blumen, T. Delany and S. Oncley, 1998: Nocturnal Boundary-layer regimes. *Bound.- Layer. Meteor.,* **88**, 255-278.

Mahrt, L. 2003: Contrasting vertical structures of nocturnal boundary layers. *Bound.-Layer Meteor.,* **105**, 351-363.

Mahrt, L. and D. Vickers, 2005a: Extremely weak mixing in stable conditions. To appear in *Bound.-Layer. Meteor.*

Mahrt and Vickers, 2005b: Formulation of turbulent fluxes in the stable boundary layer. Submitted to *J. Atmos. Sci.*

Mason, P.J and S.H. Derbyshire, 1990: Large-eddy simulation of the stably-stratified atmospheric boundary layer. *Bound.-Layer. Meteor.*, **53**, 117-162.

Merrill, J., 1977: Observational and theoretical study of shear instability in the airflow near the ground. *J. Atmos. Sci.,* **34**, 911- 921.

Miles, J.W., 1961, On the stability of heterogeneous shear flows. *J. Fluid Mech.,* **10**, 496-508.

Monin, A.S. and A.M. Obukhov, 1954: Basic laws of turbulence mixing in the surface layer of the atmosphere. *Trudy Geof. Inst. AN. SSSR.*, **24** (151) 163-187.

Nappo, C.J., 1991: Sporadic breakdown of stability in the PBL over simple and complex terrain. *Bound.-Layer Meteor.*, **54**, 9-87.

Nieuwstadt, F. T. M., 1984: The turbulent structure of the stable, nocturnal boundary layer. *J. Atmos. Sci.* , **41**, 2202 - 2216.

Oyha, Y.D., E. Neff, E.N. Meroney, 1997: Turbulence structure in a stratified boundary layer under stable conditions. *Bound.-Layer. Meteor.,* **83**, 139-161.

Poulos, G.S., W. Blumen, D.C. Fritts, J.K. Lundquist, J. Sun, S.P. Burns, C. Nappo, R. Banta, R. Newsom, J. Cuxart, E. Terradellas, B.B. Balsley, and M.L. Jensen, 2002: CASES-99: A comprehensive investigation of the stable nocturnal boundary layer. *Bull. Amer. Meteor. Soc.,* **83**, 555-581.

Pahlow, M., M. B. Parlange, and F. Porte-Agel, 2001: On Monin-Obukhov similarity in the satable amospheric boundary layer. *Bound.-Layer. Meteor.,* **99**, 225-248.

Poulos G.S., and S. Burns, 2003: An evaluation of bulk Ri-based surface layer formulation for stable and very stable conditions with intermittent turbulence. *J. Atmos. Sci*, **60**, 2523-2537.

Pristley, C.H.B., 1959: *Turbulent Transfer in the Lower Atmosphere*. University of Chicago Press, 130 pp.

Rees, J.M. and S.D. Mobbs, 1988: Studies of internal gravity waves troposphere at Halley, Antarctica. *Quart. J. Roy. Meteor. Soc.,* **114**, 939-966.

Saiki, E.M., C.H. Moeng, and P.P.Sullivan, 2000: Large-eddy simulation of the stably stratified planetary boundary layer. *Bound. -Layer. Meteor.,* **95**, 1-30.

Schumann, U. and T.Gertz, 1995: Turbulent mixing in stably stratified shear flows. *J. Appl. Meteor,* **34**, 33-48.

Shutts, G.J., M.Kitchen, and P.H. Hoare, 1988: A large amplitude gravity wave in the lower atmosphere detected by radiosonde. *Quart. J. Roy. Meteor. Soc.*, **114**, 579-594.

Smedman, A.-S.,1988: Observations of a multi-level turbulence structure in a very

stable atmospheric boundary layer. *Bound.- Layer Meteor.,* 44, 231-253.

Sorbjan, Z., 1986a: On similarity in the atmospheric boundary layer. *Bound.-Layer Meteor.,* **34**, 377 - 397.

Sorbjan, Z., 1986b: On the vertical distribution of passive species in the atmospheric boundary layer. *Bound.- Layer Meteor.*, **35**, 73-81.

Sorbjan, Z., 1986c: Local similarity of spectral and cospectral characteristics in the stable-continuous boundary layer. *Bound. -Layer Meteor.* , **35**, 257-275.

Sorbjan, Z., 1987: Comments on 'scaling the atmospheric boundary layer. *Bound.-Layer Meteor.,* **38**, 411-413.

Sorbjan, Z., 1995: Self-similar structure of the planetary boundary layer. In: *The Planetary Boundary Layer and Its Parameterization. 1995 Summer Colloquium.* Ed.: C.-H. Moeng NCAR, 525 pp., Boulder, Colorado, USA.

Sorbjan, Z., 2001: An evaluation of local similarity at the top of the mixed layer based on large-eddy simulations. *Bound. -Layer Meteor.*, **101**, 183-207.

Sorbjan, Z., 2004: Large-eddy simulations of the baroclinic mixed layer. *Bound.-Layer Meteor.,* **112**, 57-80.

Sorbjan, Z., 2005: Similarity regimes in the stably-stratified surface layer. Submitted to *Bound.-Layer Meteorology.*

Steward, R.W., 1969: Turbulence and waves in a stratified atmosphere. *Radio Sci.*, **4**, 1269-1278.

Sun, J., S. Burns, A.C. Delany, T. Oncley, A. Horst, and D. Lenschow: 2003: Heat balance in nocturnal boundary layer during CASES-99. *J. Appl. Meteor.*, **42**, 1649-1666.

Sun, J., D. Lenschow, S. Burns, R.M. Banta, R.K. Newsom, R. Coulter, S. Frasier, T. Ince, C. Nappo, B.B. Malsley, M. Jensen, L. Mahrt, D. Miller, and B.Skelly: 2004: Atmospheric disturbances that generate intermittent turbulence in nocturnal boundary layers. *Bound. -Layer Meteor.*, **110**, 255-279.

Tavoularis, S. and U. Karnik, 1989: Further experiments on the evolution of turbulent stresses and scales in uniformly sheared turbulence. *J. Fluid Mech.,* **204**, 457-478.

Turner, J.S., 1973: *Buoyancy Effects in Liquids*. Cabridge Universiy Press, 367 pp.

Van de Wiel, B.J.H., A. Moene, G. Hartogenesis, H.A. De Bruin, and A.A.M. Holtslag, 2003: Intermittent turbulence in the stable boundary layeor over land. Part III. A classification for observations during CASES-99. *J. Atmos. Sci,* **60,** 2509-2522.

Vickers, D., and L. Mahrt, 1997: Quality Control and flux sampling problems for tower and aircraft data. J.Atm.Ocean.Techn., **14**, 512-526.

Vickers, D., and L. Mahrt, 2005: A solution for flux contamination by mesoscale motions with very weak turbulence. Submitted to *Bound. -Layer Meteor*.

Yamada, T., 1975: The critical Richardson number and the ratio of the eddy transport coefficients obtained from a turbulence closure model. *J. Atmos. Sci.*, **32**, 926-933.

Wyngaard, J.C. and B. Kosovic, 1994: Similarity of structure-function parameters in the stably stratified boundary layer. *Bound.- Layer Meteor.*, **71**, 277-296.

Woods, J.D., 1969: On Richardson number as a criterion for laminar-turbulent transition in the ocean and atmosphere. *Radio Sci.*, **4**, 1289-1298.

Figure captions

Figure 1. Profiles of: (a) the temperature, and (b) the wind velocity, in the composite case W (open circles) and S (filled circles). The temperature is the deviation from the surface value.

Figure 2. Profiles of the Richardson number $\underline{Ri}$, in case W (open circles) and case S (filled circles).

Figure 3. Profiles of: (a) the heat flux, (b) the Reynolds stress, (c) the temperature variance, and (d) the vertical velocity variance, in case W (open circles) and case S (filled circles).

Figure 4. The dependence of: (a) the temperature variance, and (b) the vertical velocity variance, scaled by the "flux-based" local scales, given by Eqs. (4), on the dimensionless height z/Λ, in case W (open circles) and case S (filled circles).

Figure 5. The dependence between the dimensionless height z/Λ and the Richardson number Ri, in case W (open circles) and case S (filled circles).

Figure 6. The dependence of: (a) the heat flux, (b) the Reynolds stress, (c) the temperature variance, scaled by the "gradient-based" local scales, given by Eqs. (6), on the Richardson number Ri, in case W (open circles) and case S (filled circles).

Figure 7. The correlation coefficient $r_{w\theta}$ between the temperature and vertical velocity as the function of the Richardson number Ri, in case W (open circles) and case S (filled circles).

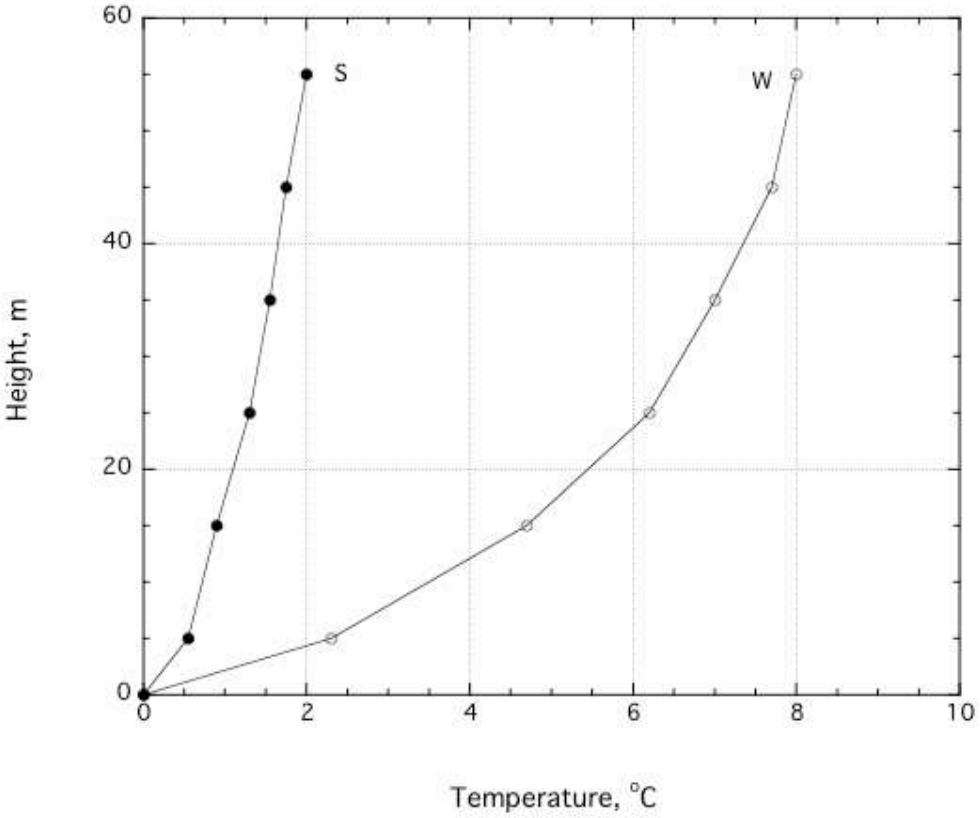

Fig.1a

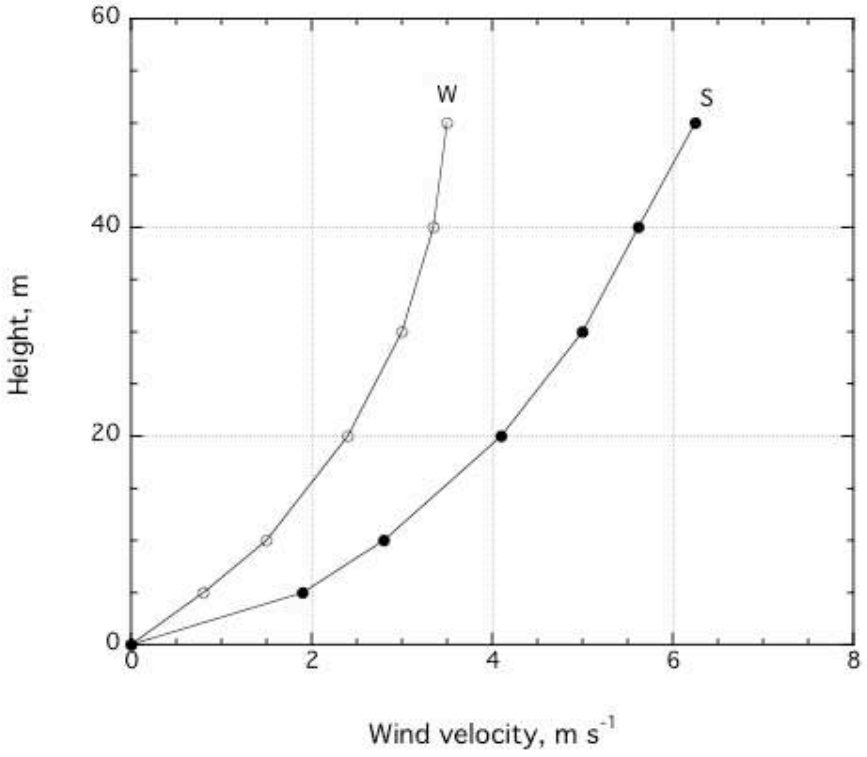

Fig.1b

Figure 1. Profiles of: (a) the temperature, and (b) the wind velocity, in the composite case W (open circles) and S (filled circles). The temperature is the deviation from the surface value.

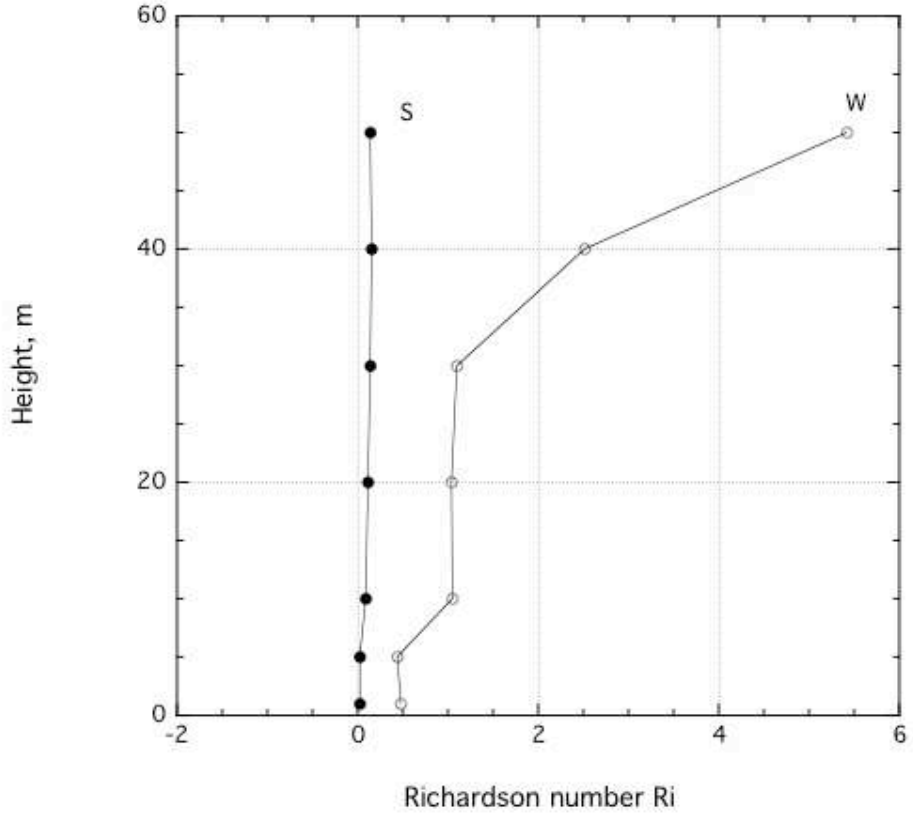

Figure 2. Profiles of the Richardson number ***Ri,*** in case W (open circles) and case S (filled circles).

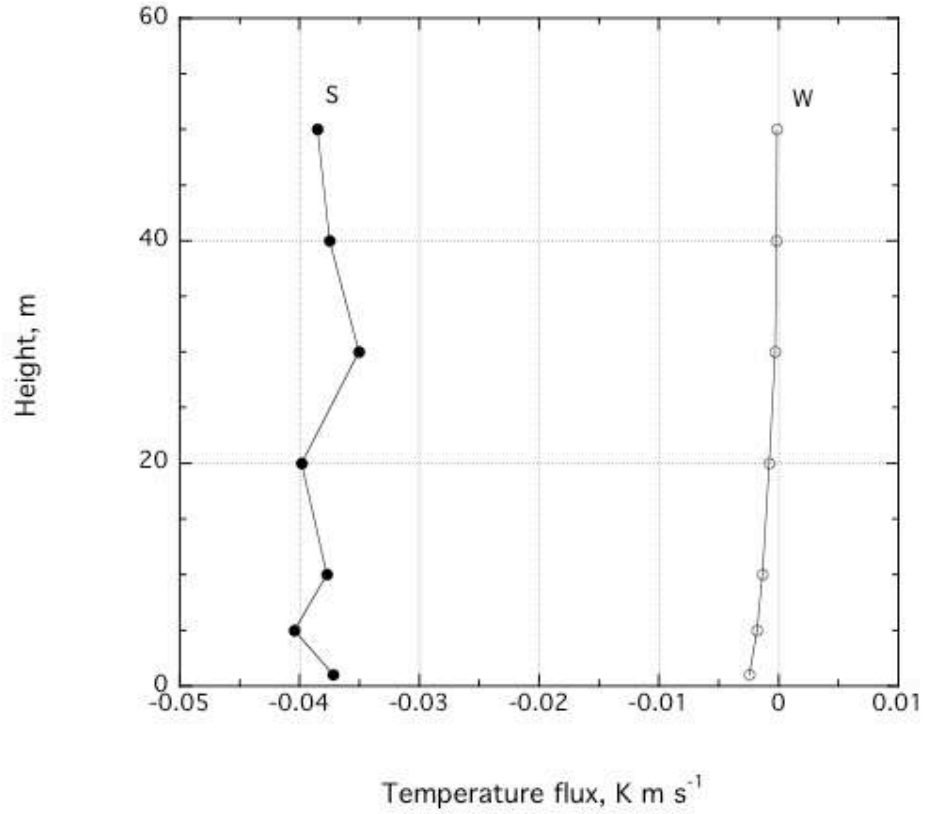
60
40
20
0
Height, m
S
W
-0.05
-0.04
-0.03
-0.02
-0.01
0
0.01
Temperature flux, K m s-1

Fig.3a

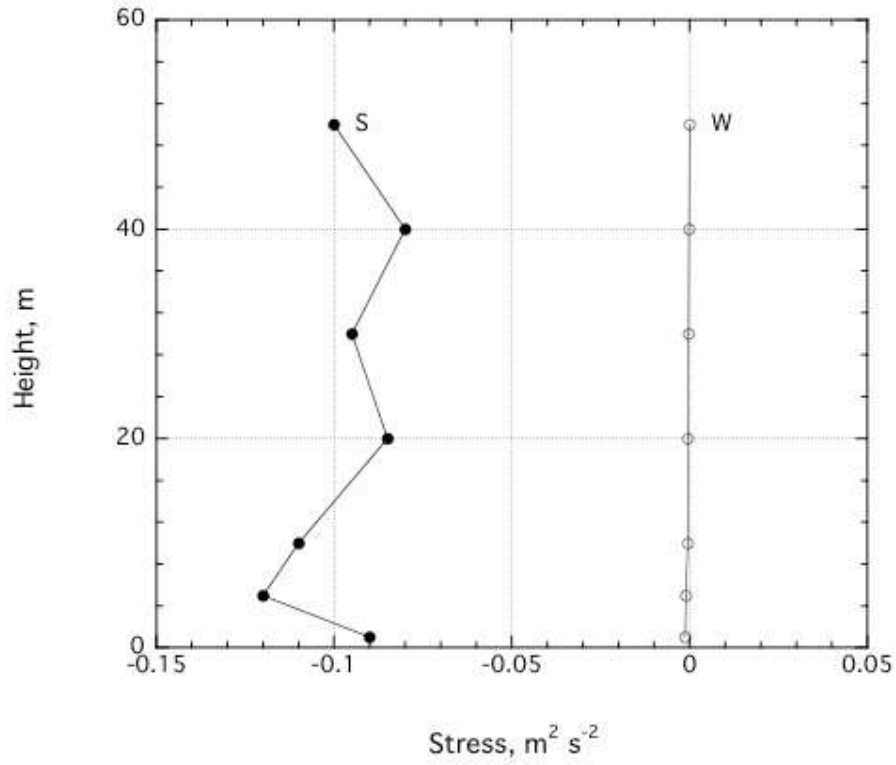

Fig. 3b

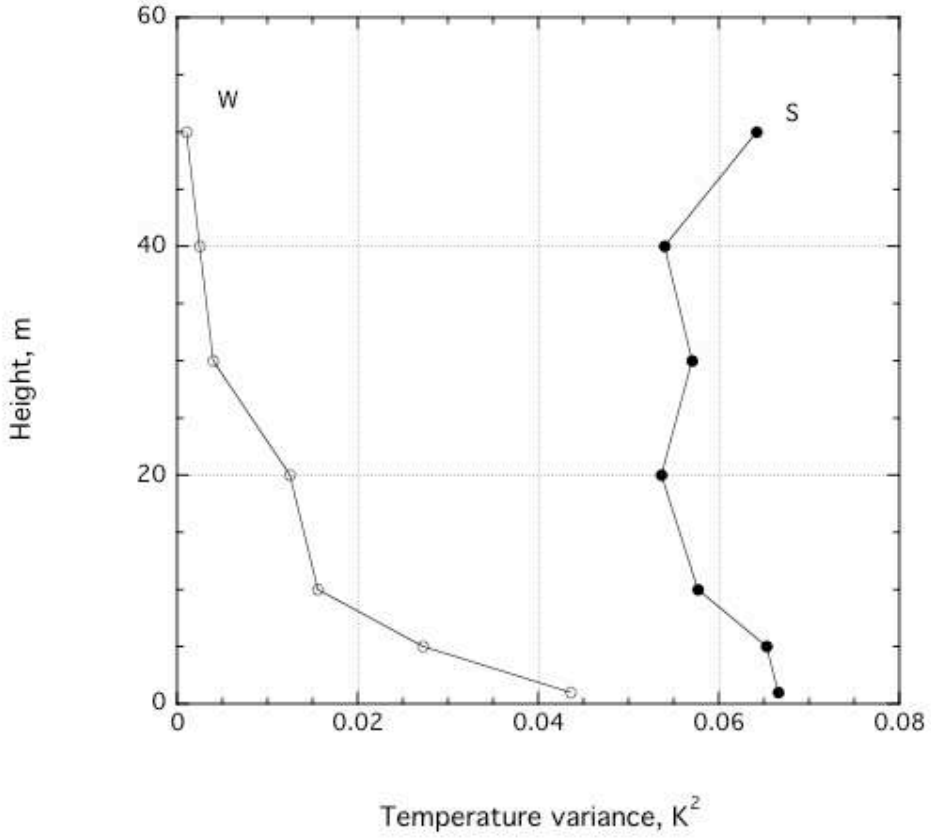
60
40
20
0
W
S
Height, m
0
0.02
0.04
0.06
0.08
Temperature variance, K2

Fig.3c

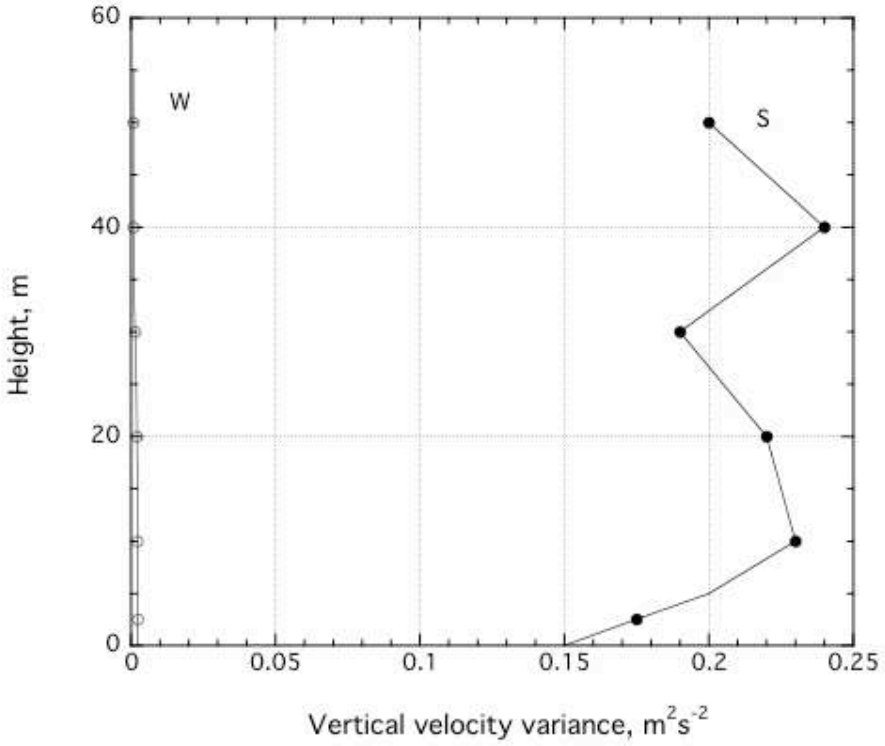

Fig. 3d

Figure 3. Profiles of: (a) the heat flux, (b) the Reynolds stress, (c) the temperature variance, and (d) the vertical velocity variance, in case W (open circles) and case S (filled circles).

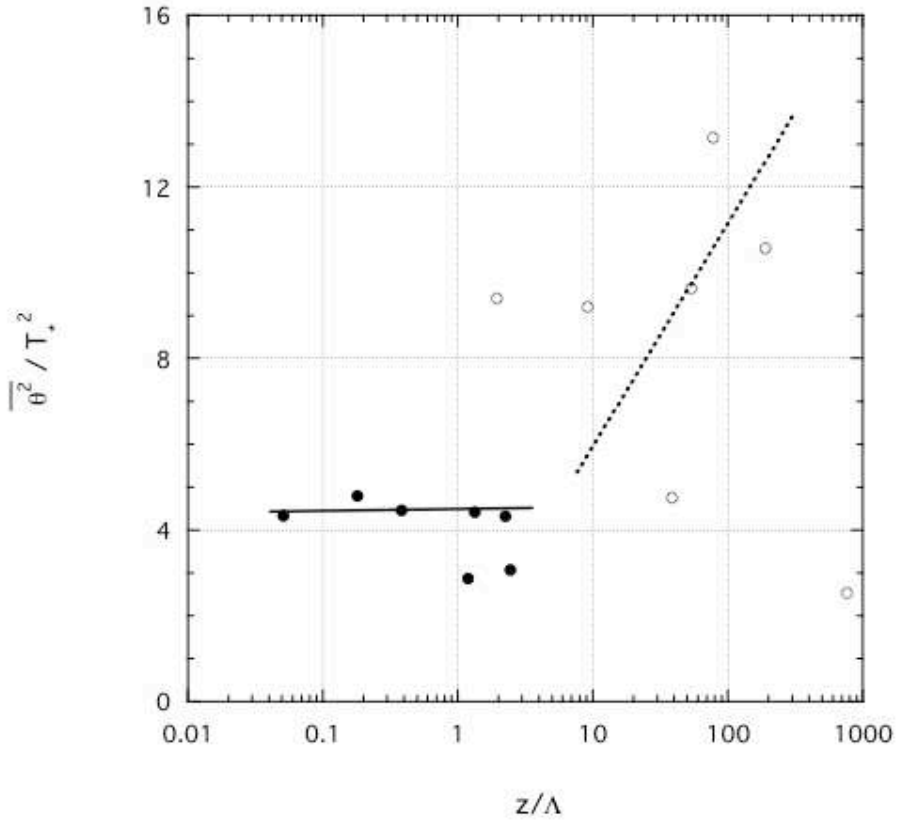

Fig.4a

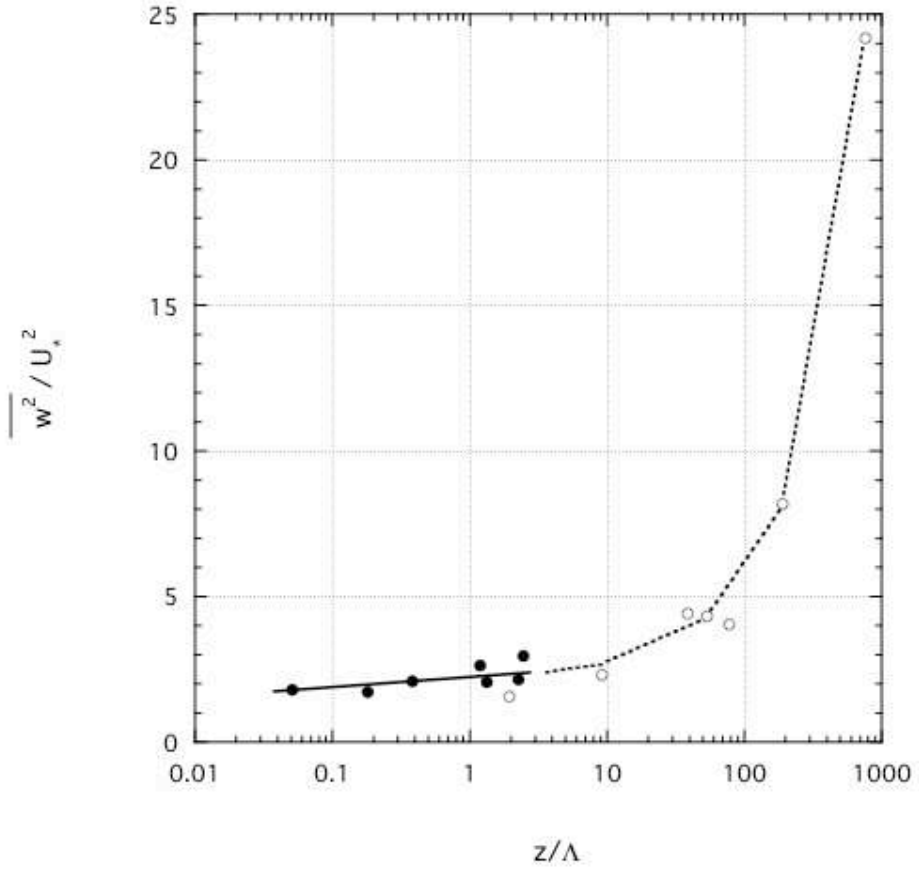

Fig. 4b

Figure 4. The dependence of: (a) the temperature variance, and (b) the vertical velocity variance, scaled by the "flux-based" local scales, given by Eqs. (4), on the dimensionless height z/Λ, in case W (open circles) and case S (filled circles).

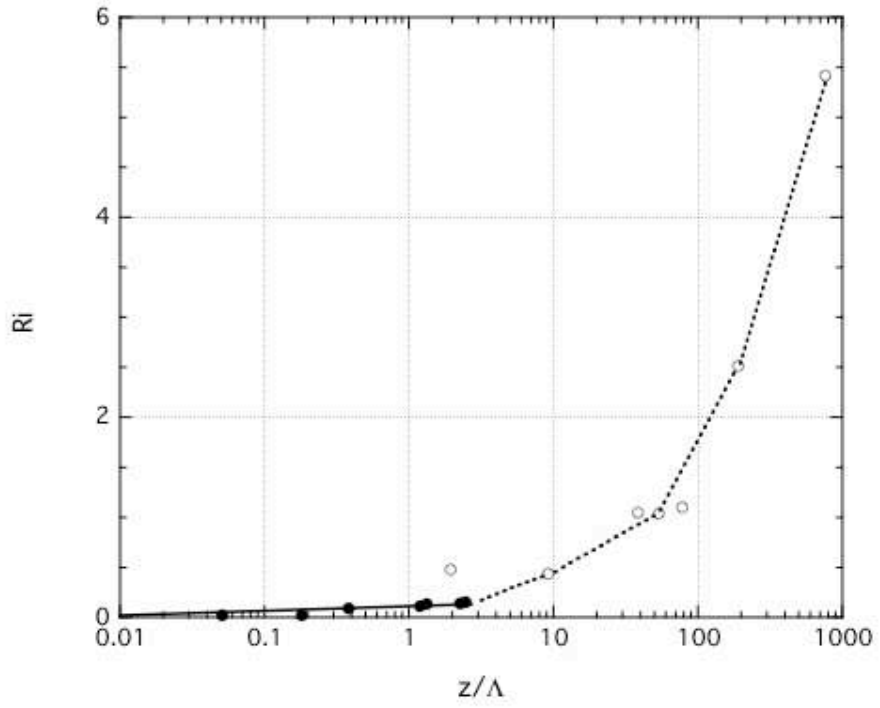

Figure 5. The dependence between the dimensionless height z/Λ and the Richardson number *Ri,* in case W (open circles) and case S (filled circles).

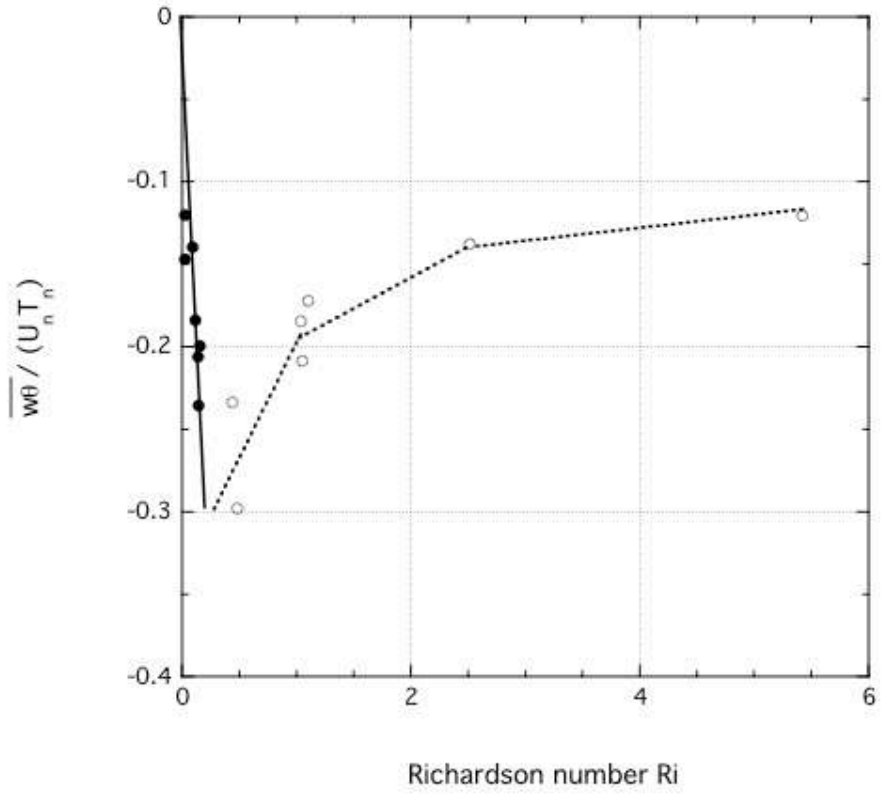

Fig.6a

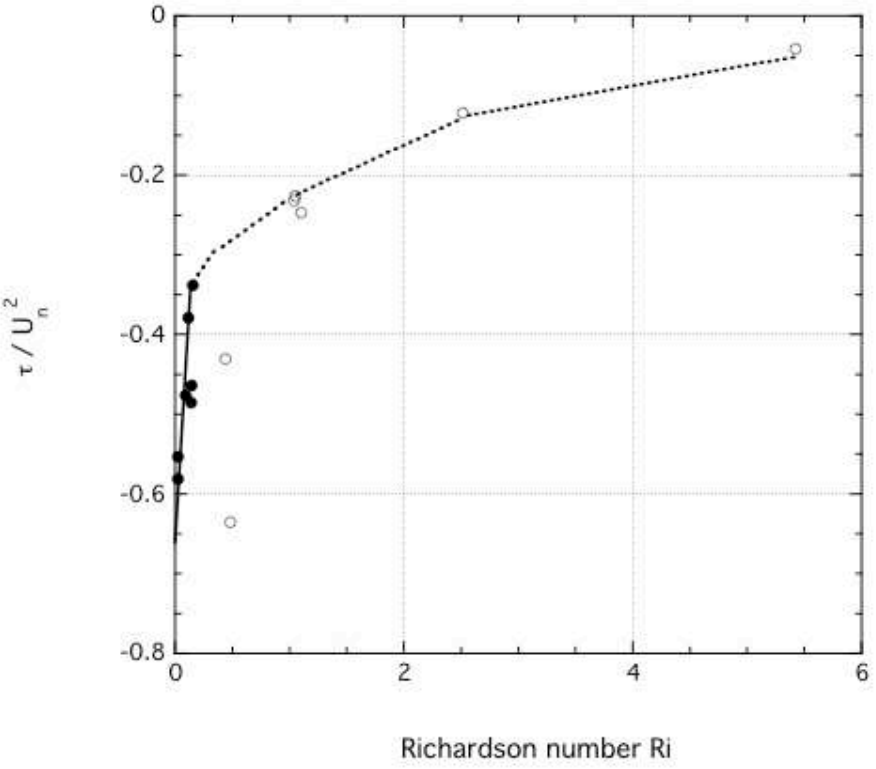

Fig.6b

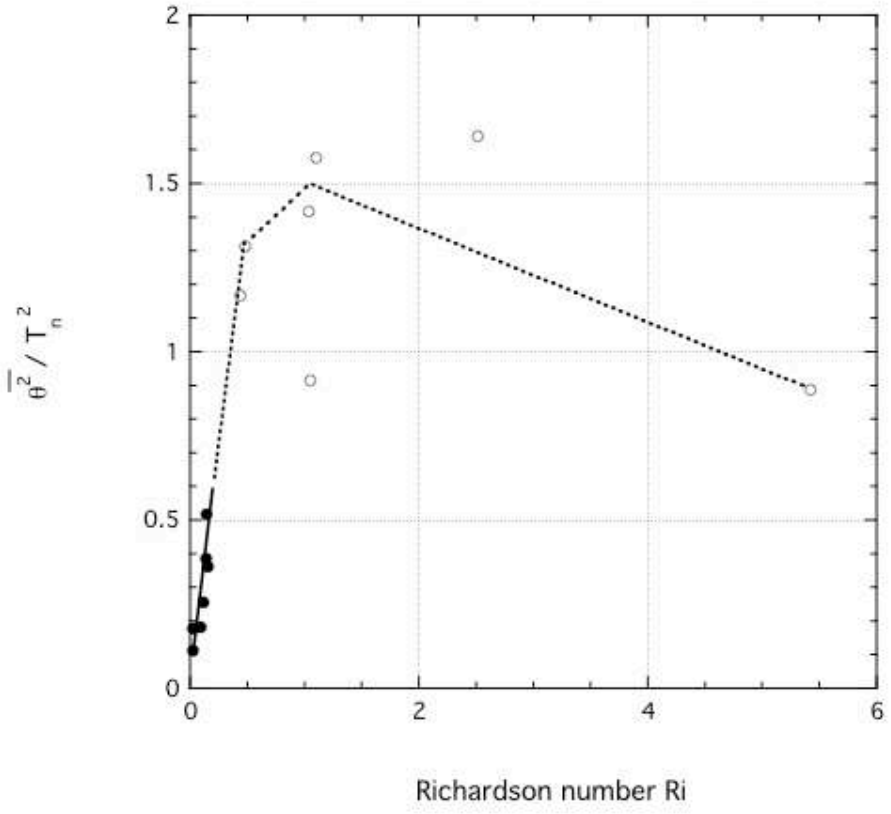

Fig. 6c

Figure 6. The dependence of: (a) the heat flux, (b) the Reynolds stress, (c) the temperature variance, scaled by the "gradient-based" local scales, given by Eqs. (6), on the Richardson number *Ri,* in case W (open circles) and case S (filled circles).

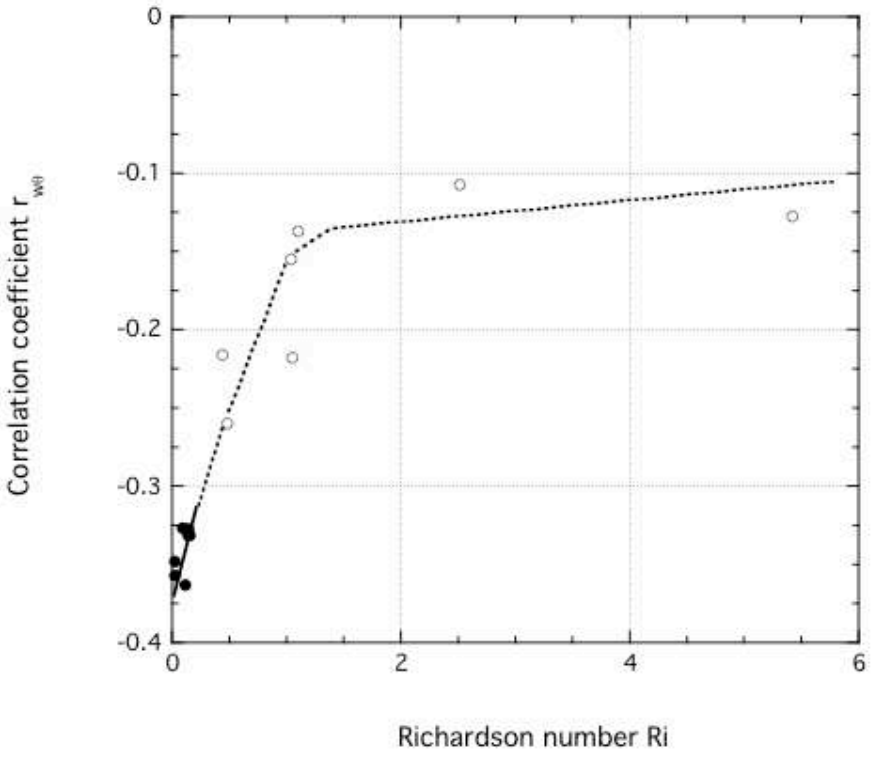

Figure 7. The correlation coefficient $r_{w\theta}$ between the temperature and vertical velocity as the function of the Richardson number *Ri*, in case W (open circles) and case S (filled circles).

TABLE 1. The surface-layer characteristics of the composite cases W and S

Composite case	No. records	u_* [m s^{-1}]	T_* [K]	H_o [K m s^{-1}]	L [m]	Net radiation [W m^{-2}]
W	22	0.04	0.07	-0.0028	0.51	-43.95
S	12	0.30	0.12	-0.0360	19.63	-56.65